AIP | The Journal of Chemical Physics

A cascade through spin states in the ultrafast haem relaxation of met-myoglobin

Cristina Consani, Gerald Auböck, Olivier Bräm, Frank van Mourik, and Majed Chergui

Citation: The Journal of Chemical Physics **140**, 025103 (2014); doi: 10.1063/1.4861467
View online: http://dx.doi.org/10.1063/1.4861467
View Table of Contents: http://scitation.aip.org/content/aip/journal/jcp/140/2?ver=pdfcov
Published by the AIP Publishing

A cascade through spin states in the ultrafast haem relaxation of met-myoglobin

Cristina Consani, Gerald Auböck, Olivier Bräm, Frank van Mourik, and Majed Chergui[a)]
Laboratoire de Spectroscopie Ultrarapide, ISIC, Ecole Polytechnique Fédérale de Lausanne, CH-1015 Lausanne, Switzerland

(Received 24 October 2013; accepted 23 December 2013; published online 13 January 2014)

We report on a study of the early relaxation processes of met-Myoglobin in aqueous solution, using a combination of ultrafast broadband fluorescence detection and transient absorption with a broad UV-visible continuum probe at different pump energies. Reconstruction of the spectra of the transient species unravels the details of the haem photocycle in the absence of photolysis. Besides identifying a branching in the ultrafast relaxation of the haem, we show clear evidence for an electronic character of the intermediates, contrary to the commonly accepted idea that the early time relaxation of the haem is only due to cooling. The decay back to the ground state proceeds partially as a cascade through iron spin states, which seems to be a general characteristic of haem systems. [http://dx.doi.org/10.1063/1.4861467]

I. INTRODUCTION

Myoglobin, the oxygen carrier in muscle tissue, is a small protein consisting of a single polypeptide chain of 153 aminoacids and an iron porphyrin (haem), as its active center. The central iron can be found in the ferric (Fe^{3+}) or the ferrous (Fe^{2+}) form and it can bind a large variety of small molecules. In metMb, a water molecule is bound to the ferric haem, which is in a high spin (S = 5/2) configuration. Crystallographic studies pointed out that in horse metMb the haem structure is almost planar, with the Fe atom not significantly displaced from the haem plane,[1] i.e., there is no or only weak doming, contrary to other high spin forms.

Although the ultrafast relaxation of photoexcited Myoglobin has been the object of intense study since the late 1980s,[2–8] the early steps of the haem photocycle are still a highly controversial issue. It is generally accepted that photoexcitation of the porphyrin is followed by an electron transfer (ET) to the iron *d*-orbitals,[6,9–13] which is believed to trigger the ligand dissociation in ferrous complexes, while in most ferric Mbs dissociation may not occur.[14–17] However, independent of the occurrence of ligand dissociation, important similarities are observed in the ultrafast dynamics (<10 ps) of the various ferric and ferrous myoglobins,[7,8,16] both with respect to spectral evolution and to time scales. Several models were proposed, all involving the porphyrin states responsible for the Q and Soret absorption (S_n^*, $n = 1, 2$) bands and two additional intermediate states called Mb_I^* and Mb_{II}^*.[3,5,7,8] Although these models differ in several aspects, they can be grouped in two main classes, depending on the assignment of the intermediates. In one case, the latter are assigned to electronically excited states which are populated either in parallel from the laser excited porphyrin states,[3] or sequentially in a cascade.[5] In the other case, Mb_I^* is ascribed to a short lived excited metal state while Mb_{II}^* is a vibrationally hot ground state (GS).

Within the last decade, not only the latter model was repeatedly supported, but also the idea developed that the details of the haem relaxation are exclusively governed by cooling and are independent of the oxidation state of the Iron atom, the nature of its axial ligand, and even of the occurrence of ligand detachment or lack thereof.[7,8,15]

Ultrafast cooling and electronic processes can be addressed by comparing the ultrafast dynamics of the system upon different excitation wavelengths λ_{exc}. In this respect, metMb is the simplest system to understand electronic relaxation in myoglobins, since the ligand does not dissociate and geminate recombination mechanisms, that could obscure haem dynamics, are absent.[14,15]

Using time-resolved fluorescence and λ_{exc}-dependent transient absorption, combined with the analysis strategies herein presented, we find that following the initial porphyrin-to-metal charge transfer, porphyrin electronic relaxation proceeds on a sub-ps time scale by back-electron-transfer (BET) from the iron orbitals. Thereafter, about 60% of the excited population directly relaxes to the ground state, where it undergoes vibrational cooling, while the remaining fraction follows a relaxation cascade through two transient states, which can be ascribed to excited electronic configurations of the iron, corresponding to different spin states of the system. We believe that our approach, based on the combination of excitation wavelength dependent, broadband transient absorption, and target analysis along with ultrafast broadband fluorescence, is very promising to distinguish the relaxation pathways in porphyrin-based systems.

The ultrafast broadband fluorescence and transient absorption setups are described in Refs. 18–21 and in the supplementary material,[45] along with the sample preparation.

a)Electronic mail: majed.chergui@epfl.ch

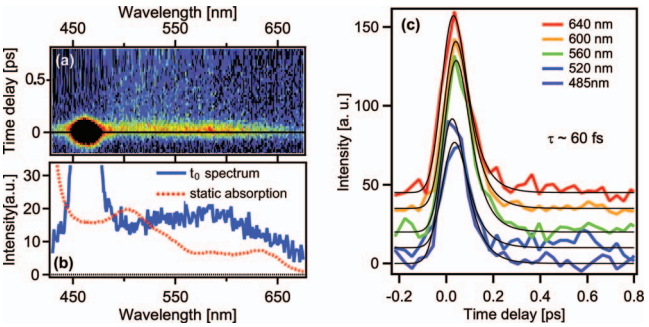

FIG. 1. Ultrafast fluorescence of metMb in the 430–670 nm spectral range, excited at 400 nm into the Soret band. (a) Time-wavelength plot of the fluorescence. The pulse-limited peak at ∼460 nm is the Raman signal from the solvent; (b) Time-zero fluorescence spectrum as extracted from the data plot in (a) (solid line). The static absorption of metMb is shown for comparison (dotted line); (c) Kinetic traces of the fluorescence at different wavelengths vertically displaced for clarity. The global analysis of these traces reveals a single exponential decay of ∼60 fs in the entire observed range.

II. RESULTS AND ANALYSIS

Fig. 1(a) shows the wavelength- and time-resolved fluorescence of metMb obtained upon excitation of the Soret band at 400 nm, together with the spectrum at time zero (panel (b)). The peak at ∼460 nm is the Raman signal of water. Soret emission is known to undergo a small Stokes shift and is thus limited to $\lambda < 470$ nm.[13,22] The broadband centred at about 580 nm appears as a mirror image of the Q band absorption which peaks at 510 nm and has a shoulder at 540 nm (see red dashed line, the absorption features at lower wavelengths were assigned to charge transfer bands[23]). It is therefore, attributed to emission of the S_1 state. Within our time resolution ((instrument response function) IRF ∼ 110 fs), it shows no rise over its entire profile, pointing to an instantaneous (<30 fs) Soret → Q band ($S_2^* \rightarrow S_1^*$) internal conversion (IC). The fluorescence kinetics can be described by a single exponential decay of ∼60 fs convoluted with the IRF (panel (c)). The mechanism causing the quenching of the haem emission is believed to be an ET from the porphyrin ring to the iron,[11,12] similar to ferrous systems.[6,9] The $S_2^* \rightarrow S_1^*$ IC is likely to occur in parallel with a direct $S_2^* \rightarrow$ Fe electron transfer, as reported for other haem proteins[13,24] and metalloporphyrins.[11]

Fig. 2 compares a set of metMb transient absorption spectra at different time delays for excitation at 400 nm (∼3.1 eV, panel (a)) and in the UV at 312 nm (∼4.0 eV, panel (b)). We also acquired data upon 288 nm (∼4.3 eV) excitation (Sec. S2 and Figure S2 of the supplementary material[45]). At this wavelength, both the haem and the two Tryptophan residues present in the protein are excited, leading to more complicated transient dynamics.[25] Analysis of the UV excitation data is available in the supplementary material,[45] and is fully consistent with the results presented here. Despite the ∼0.9–1.2 eV difference in excitation energy, the main spectral features of the transients are very similar. In the visible region, two main transient bands with excited state absorption (ESA) character are observed, centered initially around 570 nm and 440 nm and shifting progressively towards higher energies. A strong ground state bleach (GSB, negative band)

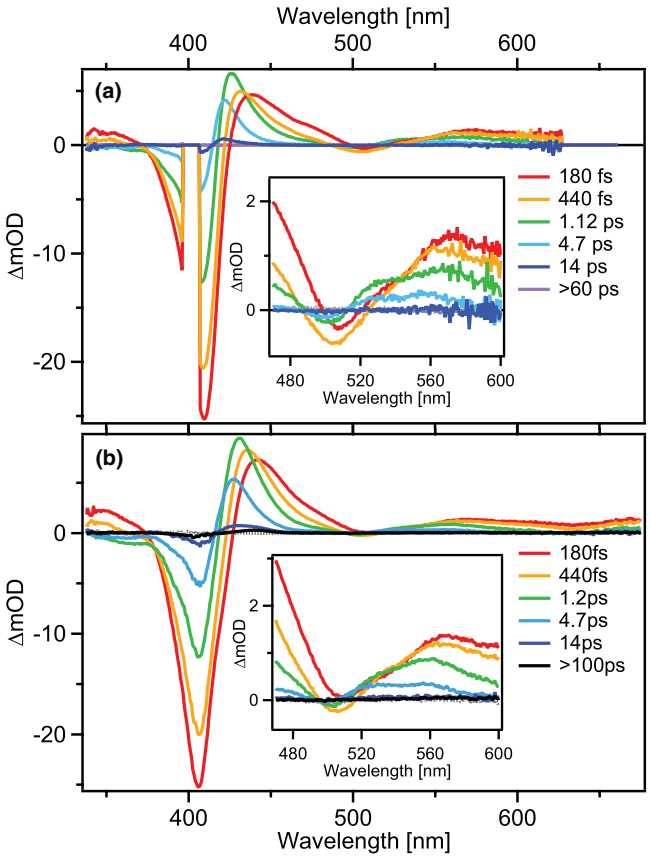

FIG. 2. Selection of transient absorption spectra at different delay times for metMb upon (a) 400 nm excitation and (b) 312 nm excitation. In panel (a), the 396–406 nm region is removed due to scattering by the pump pulse. The insets in panels (a) and (b) zoom into the Q-band region, where a transient doublet feature is observed. A more detailed view is given in the supplementary material[45] (Figure 1).

appears around 410 nm and an ESA is observed below 370 nm. A weak bleach signal, initially centered around 507 nm, is also detected both under 400 and 312 nm excitation. The shape of the TA spectra in the Soret and Q-band region agrees well with results from previous studies.[7,8] In the case of 312 nm excitation, the high optical density of the sample in the 400–418 nm region (>1.4 for a concentration corresponding to 0.2–0.3 OD at the UV excitation wavelength) and small amounts of scattered light caused a distortion in the amplitude of the signal.

All bands above 430 nm undergo a fast blue shift in the first ps, followed by an additional small blue-shift which is completed in ∼5 ps. Interestingly, a double-peaked band between 520 and 560 nm appears at times longer than 550 fs, lasting for more than 5 ps (see also insets in Figure 2) independent of the excitation energy.

For all three pump energies, the transient behavior was subject to a global analysis assuming a multi-exponential behavior (see Sec. S4 of the supplementary material[45]). Results obtained from Singular Value Decomposition (SVD) were fully confirmed by a global fit analysis (Sec. S3 of the supplementary material[45]). Four exponential components were necessary to fully describe the kinetics, whose characteristic times are given in Table I. The corresponding Decay Associated Spectra (DAS) are shown in Figure 3 of the

TABLE I. Time constants describing the evolution of the TA signal of photoexcited metMb. Reported values are the average between the results obtained with the two analysis procedures. Reported errors are 1σ.

λ_{exc} (nm)	400	312	288
τ_{S^*} (fs)	<80	<80	<80
$\tau_{Mb^*_I}$ (fs)	510 ± 10	475 ± 15	425 ± 10
$\tau_{Mb^*_{III}}$ (ps)	1.14 ± 0.03	1.07 ± 0.04	1.20 ± 0.06
$\tau_{Mb^*_{II}}$ (ps)	4.77 ± 0.05	4.66 ± 0.05	4.6 ± 0.2

supplementary material.[45] A selection of kinetic traces and their fits are reported in Figure 4 of the supplementary material.[45] Our results are in good agreement with previous experiments,[7,8] except for the ~1.1 ps dynamics, which to our knowledge was never reported before for the met form. According to the notation adopted in the literature, we refer to the ~0.5 and 4.7 ps components as arising from the Mb^*_I and Mb^*_{II} states, respectively, while we will refer to the ~1.1 ps lived state as Mb^*_{III}.

The DAS do not allow an easy assignment of the haem dynamics. For this purpose, the spectra of the intermediate species (Species Associated Spectra, or SAS) are required, which can be obtained from a target analysis. Instead of a direct fit of the experimental data to a specific decay model, we obtain the SAS from the DAS. The procedure, which is detailed here, allows us to separate the fitting of the data from the details of a specific relaxation scheme, providing a robust and fast method to test different models. For the sake of clarity, in the following treatment we will refer to all observed dynamics as coming from excited states of the system, regardless of whether they are electronic or vibrational ones.

The time dependent signal is described by a linear combination of n exponential contributions according to

$$S(\lambda, t) = \sum_{i=1}^{n} A_i(\lambda) \exp\left(-\frac{t}{\tau_i}\right), \tag{1}$$

where τ_i are the characteristic times and the pre-exponential coefficients $A_i(\lambda)$ give the DAS.

In a physically more meaningful way, the system relaxation can be described as a relaxation process through a set of N distinct states and the time-dependent signal is then given by

$$S(\lambda, t) = \sum_{j=1}^{N} n_j(t) S_j(\lambda) + [1 - n_{GS}(t)] S_{GS}(\lambda), \tag{2}$$

where S_j are the absorption spectra of each state j and $n_j(t)$ are their respective populations. The second term of (2) represents the GSB contribution, where $n_{GS}(t)$ is the time dependent GS population and $S_{GS}(\lambda)$ is the GS absorption spectrum. The time-dependent populations can be obtained by solving the system of rate equations governing the system relaxation. They are given by a linear combination of exponentials according to

$$n_j(t) = \sum_{\substack{r,m=1 \\ r \neq m}}^{l} c_{rm}(\vec{k}) e^{-\alpha_{rm} k_{rm} t}, \tag{3}$$

where the sum extends over all relaxation paths included in the model, k_{rm} is the rate for population transfer from the state r to the state m, and the coefficients α_{rm} can assume only values +1 (population decay) or −1 (rise). The specific expressions for the coefficients $c_{rm}(\vec{k})$ are determined by the model and depend on the rate constants of each relaxation step.

Since both equations (1) and (2), describe the same signal, the two right-hand sides can be equaled. The resulting equation must agree at any time, so the spectra $S_j(\lambda)$ can be calculated from the coefficients $A_i(\lambda)$ and $c_{rm}(\vec{k})$. However, while all the terms in (1) are directly obtained from the experimental data, the functions $n_j(t)$ in (2) strongly depend on how the relaxation pathway is modeled. As a consequence, the reconstructed SAS $S_j(\lambda)$ are model-dependent while the DAS are unique. For example, the same set of data can be equally well described by a simple cascade model or by a photocycle where some branching is included, yielding different reconstructed spectra. Without any further knowledge about the system, there is no way to distinguish between different models.

In the present study, we apply a rate equation model with the aim to reconstruct the absorption spectra of the intermediate states in the system relaxation, and to gain from these spectra an insight into the physical nature of these intermediates.

Our experimental results reveal the presence of three intermediate states in the haem relaxation. The easiest photocycle which can explain them is a cascade model, sketched in Figure 3, where the relaxation proceeds through all the intermediate states. In the approximation of an impulsive excitation, the system of rate equations associated with this model is

$$\begin{aligned}
n'_{S^*}(t) &= -k_{S^*1}\, n_Q(t), \\
n'_{Mb^*_I}(t) &= -k_{13}\, n_{Mb^*_I}(t) + k_{S^*1}\, n_Q(t), \\
n'_{Mb^*_{III}}(t) &= -k_{32}\, n_{Mb^*_{III}}(t) + k_{13}\, n_{Mb^*_I}(t), \\
n'_{Mb^*_{II}}(t) &= -k_{2GS}\, n_{Mb^*_{II}}(t) + k_{32}\, n_{Mb^*_{III}}(t), \\
n'_{GS}(t) &= k_{2GS}\, n_{Mb^*_{II}}(t),
\end{aligned} \tag{4}$$

with initial conditions $n_{S^*}(0) = a$, $n_{Mb^*_I}(0) = 0$, $n_{Mb^*_{III}}(0) = 0$, $n_{Mb^*_{II}}(0) = 0$, $n_{GS}(0) = 1 - a$, where the nomenclature for the populations n and rate constants k is given according to Figure 3 and a denotes the fraction of excited molecules. In the linear regime, the latter can be determined from the

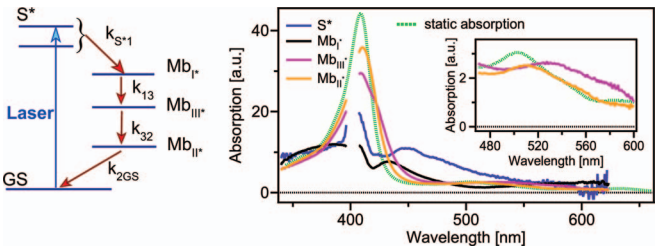

FIG. 3. Species Associated Spectra (SAS) reconstructed according to the model sketched on the left for 400 nm excited metMb. The region around 400 nm was removed because it is perturbed by scattered pump light. MetMb steady state absorption is also shown for comparison (dotted line).

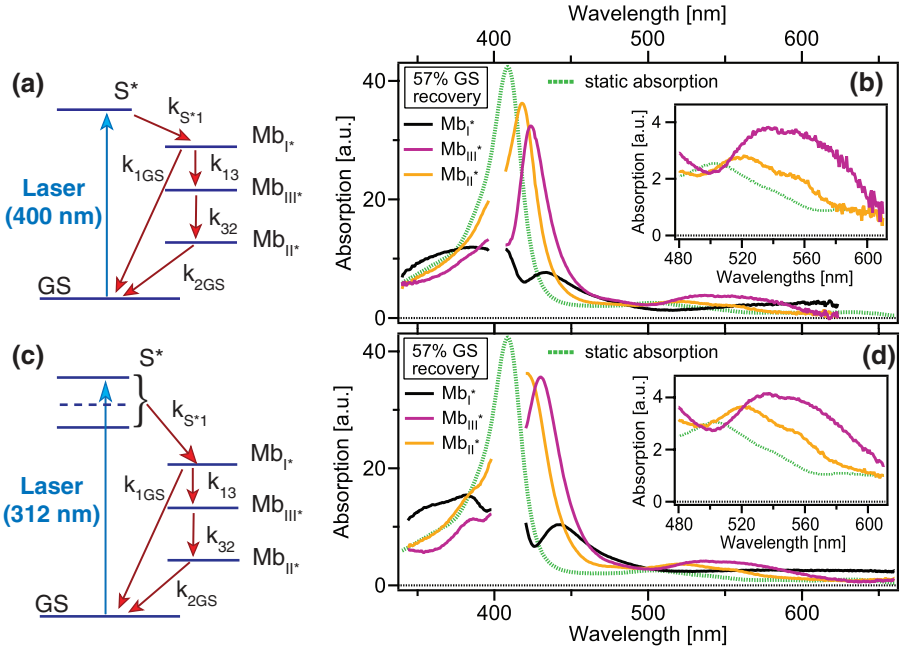

FIG. 4. (a) Model scheme for the relaxation of 400 nm excited metMb where a branching from the Mb_I^* excited state is included and (b) relative Species Associated Spectra (SAS) for a 57% direct $Mb_I^* \rightarrow$ GS recovery. The 395–405 nm region was removed due to pump scattering. (c) and (d) Same as (a) and (b) for a 312 nm excitation. The region between ~400 and 418 nm was removed because of distortions due to the high optical density of the sample.

experimental conditions as the ratio of the absorbed photons to the number of molecules in the illuminated area. In our experiments, a is estimated to be $\sim 8 \pm 1\%$ (upon 400 nm excitation; data presented here upon 312 and 288 nm excitation were scaled to the same excitation density). The rate constants are obtained from the results of the SVD and global fit analysis (as $k_{S^*1} = 16.7\ ps^{-1}$, $k_{13} = 2\ ps^{-1}$, $k_{32} = 0.87\ ps^{-1}$, and $k_{2GS} = 0.21\ ps^{-1}$). Figure 3 shows the SAS of 400 nm excited metMb derived from this model (the results for 312 nm excitation are similar and are shown in the supplementary material[45]).

The most interesting features are observed in the spectrum associated to the state Mb_{III}^*. The strongly red-shifted Q-band shows traces of a doublet structure at about 530 and 580 nm. Moreover, while the peak of the Soret band is located at 409 nm for the metMb ground state, a strong shoulder is observed on its red side at 425 nm.

In this spectrum, we recognize the presence of two species. Since the Soret band peaks in the same position as in the unexcited sample, at least part of the reconstructed absorption comes from a population in the GS. On the other hand, the red shoulder in the Soret band speaks for a hot or electronically excited state.[23] Indeed, in haem proteins the Soret band is a relatively narrow and intense feature, whose energy depends on the oxidation and spin state of the central Fe atom and on the ligands. Moreover, no other static transition appears in the GS spectrum of metMb between the Soret (409 nm) and a weak band at 467 nm, which could explain the enhanced absorption through a temperature-induced shift. Thus, the shoulder in the Mb_{III}^* SAS is indicative of the presence of an excited state with a red-shifted Soret absorption rather than a single state with two comparably intense Soret bands.

In the light of these observations, we can rule out the cascade model previously described, and we develop a second model, where the simultaneous presence of two species is accounted for by a branching from the state Mb_I^*, as sketched in Figure 4(a).

The branching ratio cannot be obtained from the time dependence of the signal, because experimentally only the sum $k_{13} + k_{1GS}$ is observed. On the basis of the previous discussion, we estimated it from the relative intensities of the GS and Mb_{III}^* Soret bands. The 22 000–26 000 cm^{-1} (384–454 nm) region of the metMb static spectrum was fitted with two Gaussians. The same spectral region of the Mb_{III}^* SAS as obtained from the above cascade model was described with three Gaussian bands, two arising from the GS population and one describing the transient Soret peak. The position of the GS bands was set to the values determined by the fit of the static spectrum. The width was allowed to be broader to account for some excess of vibrational energy on the haem, which is expected to dissipate on timescales >1 ps,[26,27] but the ratio between the respective areas was kept unchanged. The fits are shown in Figure 6 of the supplementary material.[45] If the transition strength of the Soret band is the same in the ground and transient state, the ratio between their areas is a direct estimate of the branching ratio. By calculating the ratio between the area of the red-most static and the transient Soret bands, we found that ~57% of the Mb_I^* state relaxes to the ground state, while the remaining fraction decays through the sequential path $Mb_I^* \rightarrow Mb_{III}^* \rightarrow Mb_{II}^* \rightarrow$ GS. The corresponding SAS reconstructed with this branching ratio are plotted in Figure 4(b). Now the spectra of both species, Mb_{III}^* and Mb_{II}^*, are compatible with typical myoglobin spectra. If we allow a difference of ~20% in the transition strength of the two states, the percentage of GS recovery varies by less than 10% and we do not observe significant differences in the main features of the reconstructed SAS (see Figure 7 of the supplementary material[45]). We

further analysed the effect of the uncertainty of the fitted decay time scales and the corresponding variation of the DAS on the reconstructed SAS. We find that variation of the time scales by ±3 times the uncertainty of the fitted values has only minor influence on the SAS (see also Figure 7 of the supplementary material[45]). We also analysed the transients obtained upon 312 nm excitation. The results for a pure cascade model are shown in the supplementary material,[45] and the outcome of the branching model is shown in Figure 4. These results are fully consistent with the analysis of the 400 nm excited transients.

We also evaluated an alternative model with a branching from the S* instead of the Mb_I^* state. In this case, the branching ratio for direct population of the ground state has to be assumed smaller than 20%. For larger branching ratios, ground state recovery occurs too fast resulting in partly negative amplitudes for the SAS of the Mb_I^* state, which is unphysical. For branching ratios smaller than 20%, the outcome for the SASs is very similar to the direct cascade model. Again the SAS of the Mb_{II}^* state is characterized by a double-peaked Soret band, which would in turn hint to an additional branching from the Mb_I^* state.

More complicated decay schemes with additional branchings cannot be excluded. We propose, however, the simplest model which is consistent with our data.

In summary, target analysis of the data at 400 nm excitation allows us to exclude a relaxation scheme where the three excited states are populated via a cascade and the ground state recovery occurs exclusively via Mb_{III}^*. The most plausible model, sketched in Figure 4(a), requires two competing channels in the depopulation of the Mb_I^* state, one of them leading to the (likely vibrationally hot) ground state, the other filling Mb_{III}^*. The estimated percentage of direct ground state recovery from Mb_I^* is ∼57%, and the corresponding reconstructed spectra are shown in Figure 4(b). Allowing an error of even 10%, does not lead to any significant differences in the main features of the reconstructed SAS.

Very similar results are obtained from the analysis of the transients obtained upon 312 nm (Figure 4(d)) and 288 nm excitation (see the supplementary material[45]). The percentage of direct GS recovery from the Mb_I^* state is estimated to ∼57 ± 8% and ∼55 ± 8%, upon 312 nm and 288 nm excitation, respectively, i.e., it is pump-energy independent. The peak position of the reconstructed Soret bands shows a ∼2–4 nm red-shift upon increase of the excitation energy, which is within the uncertainty of our analysis. The most pronounced effect of increase in the haem temperature is observed in the width of the Soret band, which appears significantly broader under UV excitation.

III. DISCUSSION

A. Porphyrin ground state recovery

Consistent with the time-resolved fluorescence results, we assign the <80 fs component to a porphyrin → Fe CT. The S* reconstructed spectrum (Figure 3) corresponds to the manifold of porphyrin excited states, both directly populated by laser excitation and generated by ultrafast IC (see assignment of time-resolved fluorescence results). Due to our temporal resolution, we cannot distinguish between these states.

We assign the 400–500 fs component to the recovery of the porphyrin electronic ground state via BET from the iron *d* orbitals (an overview of all relevant Fe and porphyrin molecular orbitals is given in Figure 9 of the supplementary material[45]). The SAS of the Mb_I^* state has a maximum between 430 and 450 nm and, at longer wavelengths, a broad and unstructured absorption extending beyond 650 nm. Very similar features were observed in the singlet and triplet (π, π^*) free-base and Zn-porphyrin excited states,[28] in the transients of other metallo-porphyrins,[28,29] as well as in free-base and metallo-porphyrin cations.[30–32] Within the same free-base or metallo-porphyrin compound, the singlet, triplet, and π-cation states show similar enhanced absorption on the red side of the Soret band, whose peak position differs by a few tens of nm, as well as a weak and broad absorption which extends from 500 nm to the IR. On top of the latter, a weak feature appears, which differs for the different states, as well as for different metal centers or side chains.

In a recent study[8] on oxy- and metMb, the appearance of a short-lived ($\tau \sim 500$ fs) band peaked at ∼660 nm was regarded as a signature of the ET from the porphyrin to the Fe, based on the similarities with the absorption of the porphyrin cation.

Here, we stress the striking similarities between the 400–500 fs DAS of metMb and the 150–200 fs DAS of both redox states of Cytochrome c (Cyt c) presented in Ref. 21 over the entire UV-Vis range. This is remarkable considering the different electronic structure of the three systems. In Fe(II) Cyt c porphyrin-to-iron ET is thought to populate the antibonding d_{z^2} orbital, inducing ligand detachment.[21] Instead in Fe(III) Cyt c, the electron can directly relax to a lower lying Fe-centred state, which different from the previous case, is not fully occupied. Finally, metMb is a high spin (S = 5/2) ferric compound, and its electronic configuration after ET is thus expected to be very different from that of both cytochromes. Moreover, the levels and energies of the metal-centered *d*-states are expected to be quite different for these three systems, as well as for other Myoglobin forms.[23,33]

On the basis of these latter observations and considering the common features of the 400–500 nm spectrum with other metallo- and especially free-base porphyrins in both their excited and ionic states, we exclude that the observed transient absorption arises from the Fe *d*-orbitals. Instead, we ascribe it to transitions from low-lying porphyrin states to the porphyrin HOMO. Thus, the Mb_I state can be assigned to a porphyrin$^+$-d^6 state and its decay can be seen as being due to the refilling of the porphyrin HOMO. Therefore, we can conclude that the 400–500 fs dynamics observed in metMb represents a Fe → Porphyrin BET mechanism.

B. Nature of the Mb_{III}^* and Mb_{II}^* states

The above target analysis is compatible with a branching model where, independent of the excitation energy, relaxation from the Mb_I^* state leads to ∼57 ± 8% ground state recovery. The remaining population undergoes a cascade relaxation through the Mb_{III}^* and Mb_{II}^* states. Their spectra are

quite different from that of Mb^*_I. For Mb^*_{III}, it is characterized by the typical porphyrin bands, with a Soret absorption at ~427 ± 3 nm and a double-peak Q-band at ~563 and ~530 nm. These features strongly suggest that Mb^*_{III} (and the subsequently populated Mb^*_{II}) have a ground state porphyrin configuration (compare to the spectra of porphyrin cations[34,35]), thus the Fe → porphyrin BET occurs on a 400–500 fs time scale in all the excited molecules. Therefore, the Mb^*_{III} and Mb^*_{II} states can originate either from an excited Fe electronic configuration or from a hot ground state.

We observe only very small changes in the Soret and Q-band positions and width upon increasing excess energy upon photoexcitation. This is especially apparent in the Q-band region, where the spectral evolution is less prone to additional effects of vibrational cooling compared to the Soret region due to the broader, less peaked, absorption profile. The spectra of the Mb^*_{III} and Mb^*_{II} states in this region are nearly identical for all three excitation wavelengths. They also do not appear like a simple shift and broadening of the ground state absorption but reveal a substantial change of spectral structure (the strong spectral changes on the corresponding timescales are also visible directly from the measured transient spectra without employing the SAS, see Figure 1 of the supplementary material[45]). When assuming no intermediate electronic states, these spectral changes could only be caused by structural changes at high haem temperatures resulting from the deposited vibrational energy. As a consequence, however, the effects should be enhanced at higher excitation energies and significant spectral differences would be observed, which is not the case. We thus conclude that the Mb^*_{III} and Mb^*_{II} states originate from an excited Fe electronic configuration rather than from a hot ground state. These arguments leave the different spin states of the Fe atom as the only possible candidates for the intermediate states. This assignment is also consistent with recent studies of MbN_3 where iron centered spin excited states were observed.[17]

Interestingly, the energy of the Mb^*_{III} Soret and Q bands (see also Figure 10 and Table 2 of the supplementary material[45]), as well as the double-peak structure of the Q-band, are very similar to the absorption of a 6-coordinated (6c) ferrous water bound Mb state resulting from metMb reduction at low temperatures.[36,37] The shape of the Q-band in iron-porphyrins has often been related to the redox and/or spin state of the central metal. However, many exceptions are observed:[23] For example, our results on Cyt c[13,21] showed impressive differences between the spectra of a 6- and 5-coordinated (5c) ferrous (Fe^{2+}) haem, the former being characterized by a double-peak Q-band and the latter by a broad and structureless band. The spectrum of 5c ferrous Cyt c is instead very similar to that of the 6c ferric (Fe^{3+}) protein. These observations cannot be rationalised in terms of the oxidation or the spin state of the central iron. They can, however, be explained in terms of the distribution of the electric charge on the porphyrin ring. The detachment of a ligand that acts as an electron donor induces a net decrease of the electron charge shared by the iron with the porphyrin nitrogens. We believe that this mechanism is the basis of the spectral changes in the Q-band structure of Cyt c, and, more generally, that the Q-band shape is related to the electron distribution on the porphyrin ring. This interpretation is supported by observations on the static spectra of metal porphyrins, where the substitution of porphyrin side chains induces the same effect on the Q-band structure.[28] In this context, the spectral analogies between a transient 6c Fe^{3+} metMb and a 6c Fe^{2+} metMb can be explained by a similar electronic distribution on the Fe.

Ferrous water bound Mb is a low-spin compound (S = 0) stabilized by a significant backbonding to the π^* orbitals of the macrocycle.[37] X-ray crystallography showed that there are no significant structural differences between the two water-ligated redox states. The compounds have D_{4h} symmetry and the only orbitals capable of mixing with the excited π^* porphyrin orbitals are the d_π ones, which correspond to e_g orbitals in the D_{4h} symmetry (Figure 7 of the supplementary material[45]). Thus, if the similarities between the spectra of the ferrous and ferric species are indicative of a similar electronic distribution on the haem macrocycle, this points to a similar population of the Fe d_π orbitals. In the ferrous water bound Mb, these are fully occupied. We thus assign the Mb^*_{III} state to a low-spin (S = 1/2) state where four electrons occupy the d_π orbitals.

Although we have no direct observable which allows for an assignment of the Mb^*_{II} state, we find plausible that the relaxation towards the high spin GS proceeds via an intermediate S = 3/2 electronic excited state.

Our results agree remarkably well with the findings of Lim *et al.*[5] for deoxy myoglobin (S = 2) obtained by near infrared femtosecond spectroscopy. They convincingly demonstrated the presence of an electronically excited intermediate state decaying with a time constant of 1 ps and found recovery of the electronic ground state on a timescale of 3.4 ps, providing kinetic evidence for an additional, intermediate electronic excited state. A similar recovery time for the electronic ground state (4.8 ± 1.5) for deoxy myoglobin was also obtained by Champion *et al.*[38] via a Raman technique. They observed a 1 ps decay time which agrees perfectly with the decay time of our Mb^*_{III} state and also their ground state recovery time is very close to the decay time we find for the Mb^*_{II} state. Also in the near IR spectrum of photolyzed carboxymyoglobin a feature was observed, which clearly corresponds to an electronically excited state and not a vibrational ground state, and it decays with a time constant of 240 fs.[39] This is intermediate between our observed decays with <80 fs and 500 fs but the time resolution (350 fs) of this experiment would probably not allow a separation of these two time constants.

IV. CONCLUSIONS

In summary, our data and analysis lead us to propose the photocycle shown in Figure 5 for the haem relaxation of photoexcited metMb. The ultrafast (about 60 fs) ET from the porphyrin (π, π^*) excited state manifold to the iron *d*-states is followed by a BET on a 400–500 fs time scale. Two distinct mechanisms compete in re-filling the porphyrin HOMO. While ~57% of the excited population relaxes directly to the GS, a second channel leads to population of Fe centered electronically excited states of different spin. Owing to spectral similarities between the Q-bands of the intermediate

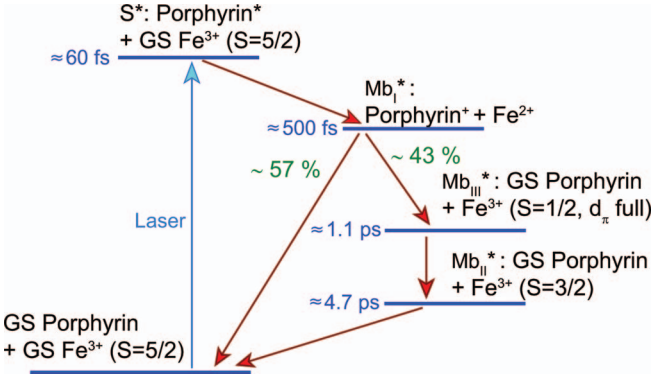

FIG. 5. Proposed photocycle for the relaxation of photoexcited metMb.

(Mb^*_{III}) state and low-spin ferrous metmyoglobin, we propose that the former is a low spin state whose d_π orbitals are fully occupied, leading to significant back-bonding to the porphyrin. We tentatively suggest that the following relaxation towards the high-spin GS proceeds through a quartet state. We think this relaxation via low lying electronic states is the dominant contribution to the observed spectral evolution while cooling of vibrational degrees of freedom has only minor effects. Ultrafast X-ray absorption spectroscopy[40,41] should be able to address this question, as was demonstrated in the case of nickeltetraphenylporphyrin[42] that has long-lived spin states.

This study provides for the first time clear evidence that the relaxation of metMb is not exclusively dominated by cooling, but involves a comparable contribution from intermediate electronic states. Moreover, the outcome of this work supports the idea that the energy and shape of the Fe-porphyrin visible spectral features (Q- and Soret bands) are strongly related to the distribution of electronic charge between the metal and the Nitrogens of the macrocycle. While the decay pathway observed here is quite specific to metMb because of its high spin (S = 5/2) GS, a photocycle passing through different spin states may be a general pattern for haem proteins and porphyrin-based compounds, as was recently reported for Fe^{III}-tetraphenylporphyrin[43] and ferric MbN_3.[17] We plan further studies on ferrous myoglobins to investigate the presence of electronic haem relaxation channels, their relation to ligand dissociation and thus, their biological relevance.

Phototriggering of biological functions has been used for decades in the case of haem proteins, which naturally function in the dark. Joffre and co-workers[44] demonstrated that, different from electronic excitation, population up to v = 6 of the CO stretch mode in carboxyhemoglobin does not trigger CO detachment despite depositing more than 1.4 eV of energy in the system.

The considerable electronic contribution to the haem relaxation in metMb is significant in this context. This electronic contribution is missing in cytochrome c,[21] where ligand detachment is not involved in the biological function. Previous studies, instead, suggested the presence of low lying, electronically excited states in the relaxation of other myoglobins. All these facts together point to the relevance of these low-lying electronic states in the actual biological function of hemo- and myo-globins, which is logical, as electronic states are the origin of chemical bonding.

ACKNOWLEDGMENTS

This work was in part supported by the NCCR MUST of the Swiss National Science Foundation (NSF(CH)). We are grateful to Dr. Andrea Cannizzo for useful suggestions and discussions.

[1]S. V. Evans and G. D. Brayer, J. Mol. Biol. **213**, 885 (1990).
[2]E. R. Henry, W. A. Eaton, and R. M. Hochstrasser, Proc. Natl. Acad. Sci. U.S.A. **83**, 8982 (1986).
[3]J. W. Petrich, C. Poyart, and J. L. Martin, Biochemistry **27**, 4049 (1988).
[4]J. W. Petrich, J.-C. Lambry, K. Kuezera, M. Karplus, C. Poyart, and J. L. Martin, Biochemistry **30**, 3975 (1991).
[5]M. H. Lim, T. A. Jackson, and P. A. Anfinrud, J. Phys. Chem. **100**, 12043 (1996).
[6]Y. Kholodenko, M. Volk, E. Gooding, and R. M. Hochstrasser, Chem. Phys. **259**, 71 (2000).
[7]X. O. Ye, A. Demidov, F. Rosca, W. Wang, A. Kumar, D. Ionascu, L. Y. Zhu, D. Barrick, D. Wharton, and P. M. Champion, J. Phys. Chem. A **107**, 8156 (2003).
[8]S. Ishizaka, T. Wada, and N. Kitamura, Photochem. Photobiol. Sci. **8**, 562 (2009).
[9]F. Adar, M. Gouterman, and S. Aronowitz, J. Phys. Chem. **80**, 2184 (1976).
[10]B. Steiger, J. S. Baskin, F. C. Anson, and A. H. Zewail, Angew. Chem., Int. Ed. **39**, 257 (2000).
[11]S. Sorgues, L. Poisson, K. Raffael, L. Krim, B. Soep, and N. Shafizadeh, J. Chem. Phys. **124**, 114302 (2006).
[12]M. H. Ha-Thi, N. Shafizadeh, L. Poisson, and B. Soep, Phys. Chem. Chem. Phys. **12**, 14985 (2010).
[13]O. Bräm, C. Consani, A. Cannizzo, and M. Chergui, J. Phys. Chem. B **115**, 13723 (2011).
[14]W. X. Cao, J. F. Christian, P. M. Champion, F. Rosca, and J. T. Sage, Biochemistry **40**, 5728 (2001).
[15]X. Ye, A. Demidov, and P. M. Champion, J. Am. Chem. Soc. **124**, 5914 (2002).
[16]J. Helbing, L. Bonacina, R. Pietri, J. Bredenbeck, P. Hamm, F. van Mourik, F. Chaussard, A. Gonzalez-Gonzalez, M. Chergui, C. Ramos-Alvarez, C. Ruiz, and J. Lopez-Garriga, Biophys. J. **87**, 1881 (2004).
[17]J. Helbing, Chem. Phys. **396**, 17 (2012).
[18]A. Cannizzo, O. Bräm, G. Zgrablic, A. Tortschanoff, A. A. Oskouei, F. van Mourik, and M. Chergui, Opt. Lett. **32**, 3555 (2007).
[19]G. Zgrablić, K. Voïtchovsky, M. Kindermann, S. Haacke, and M. Chergui, Biophys. J. **88**, 2779 (2005).
[20]C. Consani, M. Prémont-Schwarz, A. Elnahhas, C. Bressler, F. van Mourik, A. Cannizzo, and M. Chergui, Angew. Chem., Int. Ed. **48**, 7184 (2009).
[21]C. Consani, O. Bräm, F. van Mourik, A. Cannizzo, and M. Chergui, Chem. Phys. **396**, 108 (2012).
[22]U. Tripathy, D. Kowalska, X. Liu, S. Velate, and R. P. Steer, J. Phys. Chem. A **112**, 5824 (2008).
[23]*Iron Porphyrins*, edited by A. B. P. Lever and H. B. Gray (Addison-Wesley, Reading, MA, 1983), Part 1.
[24]P. M. Champion and G. J. Perreault, J. Chem. Phys. **75**, 490 (1981).
[25]C. Consani, G. Auböck, F. van Mourik, and M. Chergui, Science **339**, 1586 (2013).
[26]T. Kitagawa, N. Haruta, and Y. Mizutani, Biopolymers **67**, 207 (2002).
[27]S. G. Kruglik, J. C. Lambry, J. L. Martin, M. H. Vos, and M. Negrerie, J. Raman Spectrosc. **42**, 265 (2011).
[28]J. Rodriguez, C. Kirmaier, and D. Holten, J. Am. Chem. Soc. **111**, 6500 (1989).
[29]X. Zhang, E. C. Wasinger, A. Z. Muresan, K. Attenkofer, G. Jennings, J. S. Lindsey, and L. X. Chen, J. Phys. Chem. A **111**, 11736 (2007).
[30]J. Fajer, D. C. Borg, A. Forman, D. Dolphin, and R. H. Felton, J. Am. Chem. Soc. **92**, 3451 (1970).
[31]Z. Gasyna, W. R. Browett, and M. J. Stillman, Inorg. Chem. **24**, 2440 (1985).
[32]C. K. Chang, L. K. Hanson, P. F. Richardson, R. Young, and J. Fajer, Proc. Natl. Acad. Sci. U.S.A. **78**, 2652 (1981).
[33]M. Zerner and M. Gouterma, Inorg. Chem. **5**, 1707 (1966).

[34]R. H. Felton, D. Dolphin, D. C. Borg, and J. Fajer, J. Am. Chem. Soc. **91**, 196 (1969).
[35]D. Dolphin and R. H. Felton, Acc. Chem. Res. **7**, 26 (1974).
[36]D. C. Lamb, A. Ostermann, V. E. Prusakov, and F. G. Parak, Eur. Biophys. J. **27**, 113 (1998).
[37]N. Engler, A. Ostermann, A. Gassmann, D. C. Lamb, V. E. Prusakov, J. Schott, R. Schweitzer-Stenner, and F. G. Parak, Biophys. J. **78**, 2081 (2000).
[38]P. Li, J. T. Sage, and P. M. Champion, J. Chem. Phys. **97**, 3214 (1992).
[39]M. H. Lim, T. A. Jackson, and P. A. Anfinrud, *Ultrafast Phenomena VIII*, Springer Series in Chemical Physics **52**, 552 (1993).
[40]C. Bressler, C. Milne, V.-T. Pham, A. El Nahhas, R. M. van der Veen, W. Gawelda, S. Johnson, P. Beaud, D. Grolimund, M. Kaiser, C. N. Borca, G. Ingold, R. Abela, and M. Chergui, Science **323**, 489 (2009).
[41]F. A. Lima, C. J. Milne, D. C. V. Amarasinghe, M. H. Rittmann-Frank, R. M. van der Veen, M. Reinhard, V.-T. Pham, S. Karlsson, S. L. Johnson, D. Grolimund, C. Borca, T. Huthwelker, M. Janousch, F. van Mourik, and M. Chergui, Rev. Sci. Instrum. **82**, 063111 (2011).
[42]L. X. Chen, X. Zhang, E. C. Wasinger, K. Attenkofer, A. Z. Jennings, G. Muresan, and J. S. Lindsey, J. Am. Chem. Soc. **129**, 9616 (2007).
[43]A. S. Rury and R. J. Sension, Chem. Phys. **422**, 220 (2013).
[44]C. Ventalon, J. M. Fraser, M. H. Vos, A. Alexandrou, J. L. Martin, and M. Joffre, Proc. Natl. Acad. Sci. U.S.A. **101**, 13216 (2004).
[45]See supplementary material at http://dx.doi.org/10.1063/1.4861467 for details on the experimental procedures, a description of the global analysis procedure, supplementary figures and tables on data analysis and the data upon 288 nm excitation.